

## **EVALUATION OF PROCESSING VARIABLES IN LARGE AREA POLYMER SINTERING OF SINGLE LAYER COMPONENTS**

**By: Justin Nussbaum<sup>1</sup>, Garrett Craft<sup>2</sup>, Julie Harmon<sup>2</sup>, Nathan Crane<sup>1</sup>**

**<sup>1</sup>Department of Mechanical Engineering, University of South Florida, Tampa, FL 33610**

**<sup>2</sup>Department of Chemistry, University of South Florida, Tampa, FL 33610**

### **ABSTRACT**

As the additive manufacturing (AM) industry continues to boom, the material palette continues to grow. However, the materials applicable to selective laser sintering (SLS) remains limited. Typically, the scanning laser beam heats each location for milliseconds at a time with a very high heating flux followed by quick cooling. This can create large temperature gradients and high local temperatures. Many polymers will degrade or fail to densify under these conditions. Due to the economic constraints for point processing, little work has been done to evaluate the sintering process with lower intensities, longer exposure times and larger areas than are typical with conventional SLS. We will report on a new method for simultaneously heating large areas with spatially-controlled heat flux. A demonstration system and test material is presented and characterized. It is then used to evaluate the relationships between heating rates, exposure time, and resulting sintering levels for traditional Nylon 12 powders in single layer parts.

### **INTRODUCTION**

Additive manufacturing (AM) is a rapidly growing field [1]. Besides making prototypes, the applications are expanding into the electronics, medical, aerospace, military and manufacturing industries [1-4]. The requirements from these industries have a large amount of variation depending on the application. AM is a great candidate for meeting these needs because of its capability to make parts with complex geometries, in many materials and with a high degree of customization [5].

Additive manufacturing (AM) is an industrial manufacturing method used to create 3D components from solid digital computer models. The components are sliced into 2D cross sections of a prescribed thickness. Each 2D cross section is then reproduced from the feedstock material with exceptional accuracy. These 2D cross sections are stacked on top of each other and fused to the layer beneath it, creating components with complex 3D geometry. The layering nature of AM allows each part to be unique without requiring custom tooling but at the cost of fabrication time [5].

Selective laser sintering (SLS) is an additive manufacturing method that produces high quality parts suitable for end-use. Similar to most other additive manufacturing technologies, SLS forms a part by fusing together multiple layers. To form 3D objects with SLS, a focused laser is typically used to impart energy into a preheated powder bed, fusing together the particles in the exposed area. A single area is typically exposed for milliseconds [6-8] at a time as a laser scans a 2D cross section of the part to be created. A new layer of powder is then deposited on top of the first and the process repeats as shown in Figure 1 below.

During the few milliseconds of exposure, the powder particles are brought well above their melting temperature which requires high heating rates. In the case of plastics this can cause sensitive materials to degrade as some parts of the material will be significantly hotter than others. Additionally, the best SLS materials are partially crystalline with a well-defined melting point [9, 10]. This allows the powder to be preheated near the melting point without the powder bed fusing together and reduces the difficulty of spreading new uniform layers. Furthermore, the material should have minimal degradation during transient heating or under prolonged preheat in the powder bed. Part distortion can also be reduced if the crystallization temperature is well below the melting point [11]. Nylon is currently one of a few select materials which have properties that make it suitable for laser sintering. A vast majority of the materials used for SLS are nylons or nylon-based because of these constraints [12].

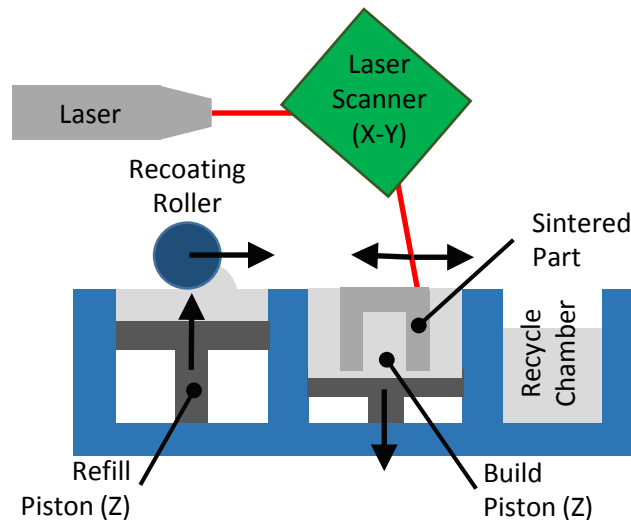


Figure 1 – During the SLS process a laser and laser scanner sinters the powder in the X-Y axis while the recoating roller and refill piston supplies powder for a new layer.

Typically, SLS systems are composed of a high power laser, a galvanometer for steering the laser and a powder spreading system contained within a hermetically sealed inert environment. This leads to relatively expensive and complex systems, putting this out of range for most users [1]. In order to produce parts economically with high spatial resolution, commercial systems generally have a small laser diameter (~0.5 mm) with high scanning speeds (~1-5 m/s) [6-8]. The proposed system is an alternative to SLS which will provide a lower initial cost and is capable of selectively sintering an entire layer of powder in a single exposure using a high power projection system.

### Effects of Viscosity

High temperatures and heating rates can degrade some polymeric materials [13, 14]. Chain scission and oxidation can damage polymer chains and reduce performance by affecting chain molecular weight and stability [14]. Additionally, post condensation reactions in the bulk phase at elevated temperatures can cause increases in the molecular weight in unmodified polyamide (nylon). Thus affecting melt viscosity and sintering efficacy.

Polymer sintering typically occurs through a viscous sintering process. It is a two stage process involving the coalescence of powder particles followed by porosity shrinkage and removal. The early phases are described by a simple viscous sintering model developed by Frenkel as seen below in Equation 1 [15]. Liquid phase sintering is driven by surface tension forces which attempts to minimize surface energy by reducing the surface area [10]. As viscosity is a measure of the resistance to flow, in order to fully fuse and coalesce these particles, the polymer must have sufficiently low viscosity to allow the material to flow over the required sintering time [16]. Low strength components with high porosity will result if viscosities are too high or heating times are too short during sintering. During the transition from solid to liquid, the viscosity drastically decreases, allowing the material to flow. In the simple viscous sintering model below, it becomes evident that the zero shear viscosity has a large impact in sintering coalescence by:

$$\frac{x}{r} = \left( \frac{3\gamma}{2\eta_0 r} \right)^{1/2} t^{1/2} \quad (1)$$

Where x is the joint length of particle coalescence relative to the original radius (r),  $\gamma$  is the surface tension,  $\eta_0$  is the zero shear viscosity and t is the sintering time. The sintering rate is determined by the material viscosity. Specifically, the zero shear rate which is most relevant because of the relatively low flow velocity experienced during sintering creates minimal shear stresses. Zero shear viscosity is proportional to the weight averaged molecular weight and is therefore sensitive to the effects of post condensation reactions that increase the molecular weight [17]. However, the low exposure time and high heating rates in SLS create highly transient, position-dependent temperatures. This makes it difficult to control the viscosity in-situ or tune the process conditions to the material properties. For laser sintering the easiest way of modifying the zero shear viscosity is by adjusting the molecular weight of the material [15]. Furthermore, the molecular weight is an intrinsic material property which increases over time during the preheat and sintering stages, making in-situ control of this property difficult as well. In the proposed projection sintering system the powder is sintered over the course of a few seconds allowing more time for in-situ monitoring and control.

### **Projection Sintering**

This paper describes a system capable of sintering single layered parts with a single exposure and evaluates the parts produced by this method. This concept, of a selective single large area exposure can be seen below in Figure 2. The test system uses a well-established recoating method commonly used in SLS machines where a blade is used to spread new uniformly smooth layers. However, in this approach, the laser has been replaced by a high intensity projector. The off-the-shelf projector in this study has been modified to concentrate 7.3 W of optical power onto a 3.7 cm<sup>2</sup> exposure area while also boosting the optical power. The projection system exposes and sinters an entire layer simultaneously over the course of a few seconds. This method allows for

longer exposure times without compromising the overall build time. This may also enable improved properties for sintering of a wider variety of materials.

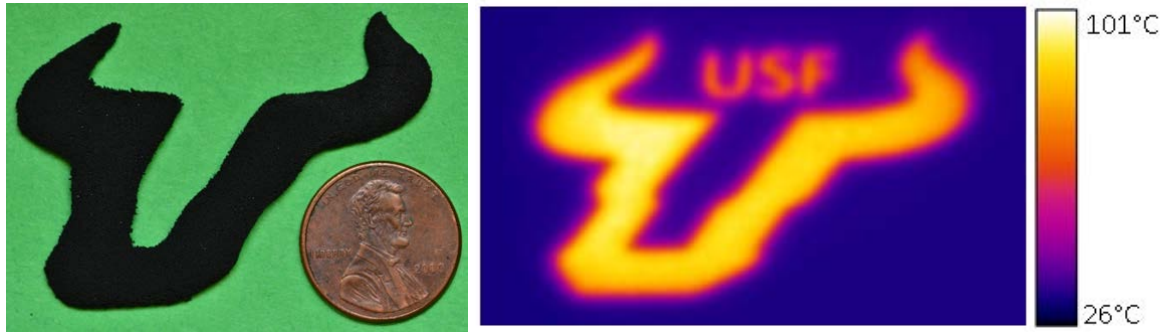


Figure 2 – left) example part created with a single, large area exposure, right) example thermal image of the University of South Florida logo on a nylon 12 powder bed created with projection sintering system

### **EXPERIMENTAL SETUP FOR PROJECTION SINTERING**

To create parts with this system, powder was evenly distributed onto an aluminum platform. A blade was used to spread a layer of powder 1.5 mm thick. A thermocouple was placed in the center of the platform halfway through the thickness of the powder. This thermocouple was used to monitor the temperature of the powder to maintain a preheat temperature of 170 °C. A laboratory convection oven was then placed on its back and the platform and powder were placed on a wire platform inside the oven. A borosilicate glass window was placed in the door of the oven for images to be projected onto the preheated powder inside the oven from the projector mounted outside of the heated chamber. The interior of the oven was subjected to standard atmospheric conditions rather than an inert nitrogen environment which is typical of SLS machines. A schematic of the test system is presented below in Figure 3.

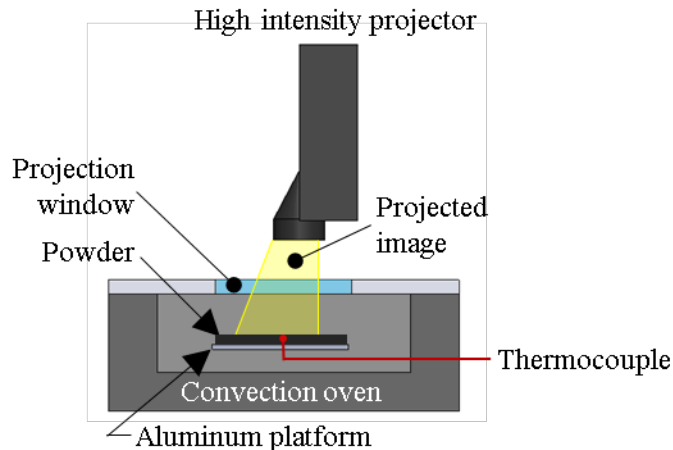


Figure 3 – In this experimental setup for polymer powders, an aluminum plate holds a 1.5mm layer of nylon powder at a preheat temperature in an oven. A thermocouple in the center of the powder is used to select the proper preheat temperature while the high power projector exposes and sinters the powder through a borosilicate glass window.

Since this study seeks to understand the interaction between exposure time and intensity these variables must be carefully controlled and their accuracy validated. A white image on a black background was sent to the projector through Microsoft PowerPoint and the corresponding image was projected onto the powder. White pixels represent areas which are receiving the maximum power while black pixels contain the least amount of intensity. Depending on the level of gray scale, varying levels of power can be projected.

In order to determine the proper preheat temperature, a differential scanning calorimetry (DSC) study was conducted on the PA2202 with a TA SDT Q600. This DSC study was conducted in an air environment with a heating and cooling rate of 10°C/min. The powder was first dried in roughing vacuum at 70°C for 24 hours. The DSC data (shown below in Figure 4) shows that a phase transition begins around 175°C. This corresponds well with the manufacturer's reported melting temperature of 172-180°C [18]. On cooling, crystallization begins below 155 °C. To maintain a temperature directly under the melting temperature, a 170°C power preheat temperature was chosen. By preheating the powder to just under the melting temperature, less optical energy is required to melt the powder and reduces the amount of internal stresses which can lead to warping.

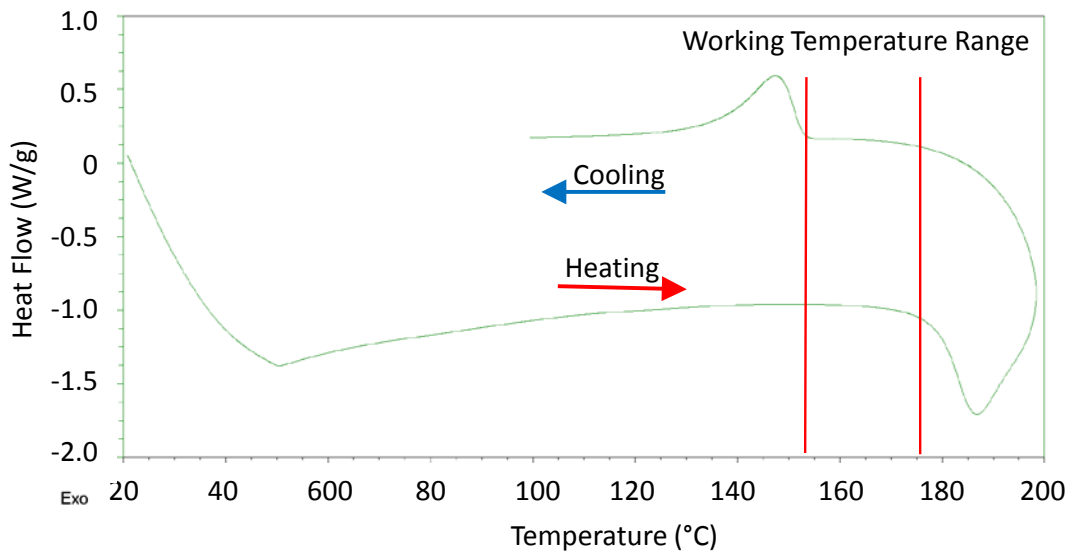


Figure 4 Differential scanning calorimetry study shows a solid to liquid phase transition at ~175°C. A preheat temperature was chosen 5°C below this transition at 170°C..

### Optical Power

An Optoma X316 off-the-shelf projector was modified to decrease the exposure area from a maximum of 278,709 cm<sup>2</sup> to 3.7 cm<sup>2</sup>. Since the maximum optical power (W) is fixed and independent of screen size, decreasing the screen size increases the power density (W/cm<sup>2</sup>). Additionally, the optical power was boosted from 1.8 W to 7.3 W, measured from a fully white projected image on a Thorlabs S310C thermal power sensor. Overall, this provides a power density increase from 6.5x10<sup>-6</sup> W/cm<sup>2</sup> to 1.97 W/cm<sup>2</sup>, an increase of more than 30,000%.

The projector's optical power is provided by a 190 W ultra-high pressure mercury vapor (UHP) bulb. UHP bulbs produce a broad spectrum of light that ranges from the ultra violet (UV) to infrared (IR) spectrum. A majority of the energy from UHP bulbs are contained within the visible spectrum (400-800 nm) and produces a mostly white light. The absorption of visible light is strongly connected to the color of the absorbing material. As such, white powders reflect most of the visible light away from the surface, absorbing only a small portion of the optical energy from the light. A dark colored powder absorbs a much larger quantity of energy from the light. In order to maximize the absorbed energy from the light, a dark gray nylon 12 powder (PA2202) produced by EOS was selected for testing. This differs from SLS systems which use a CO<sub>2</sub> laser operating in the IR spectrum at 10.6 μm, where energy absorbance is not heavily color dependent as it is with visible light. Upon melting, the PA2202 powder becomes evenly black as the black pigment (carbon black) evenly disperses through the component. This material is manufactured for the SLS industry and is commonly used in SLS systems to create black components.

The degree of sintering is highly influenced by the amount of time the powder is exposed to high intensity light. A high degree of timing accuracy is required by the system in order to create reproducible results. The timing accuracy of the system was measured by projecting an image onto a high speed photodiode (OPT101 produced by Texas Instruments) which also internally contains a transimpedance amplifier. The photodiode was connected to an Agilent Technologies Mixed Signal Oscilloscope (MSO6012A) capable of 100 MHz sampling frequencies. An image was displayed then removed after a specified animation time and the photodiode output was recorded. The system occasionally produced images for less or more than the specified time. This amount of error lead to a timing inaccuracy of  $1\text{ms} \pm 27\text{ms}$ . Since exposure times ranged from 1-15s during testing, this amount of error in the exposure time was considered negligible.

One issue identified from using PowerPoint shapes was that varying levels of grayscale were not linearly proportional to the projected power. By using a Thorlabs S310C thermal power meter, varying levels of grayscale were projected and the power contained within the light was measured by allowing the power meter to reach steady state. This test was conducted three times and the results are shown below in Figure 5. By fitting a regression line to the data, the projected power could be calibrated.

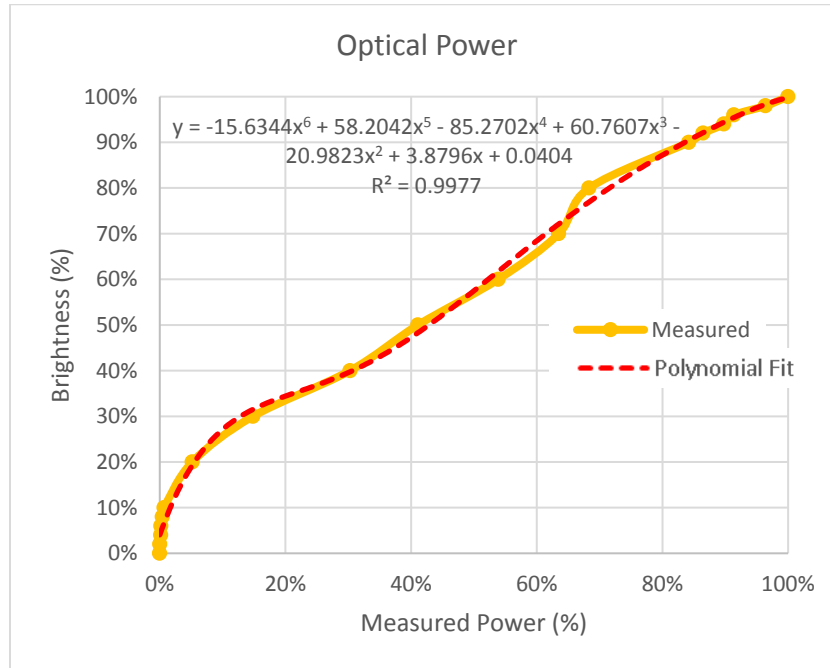


Figure 5 – Optical power as measured by thermal power sensor relative to the desired output capability was mapped to different levels of brightness. A brightness of 100% indicates the highest power and is completely white, while an intensity of 0% is the lowest intensity and is completely black.

As the light is emitted from the projector onto the powder, some of the light is absorbed, some of it is reflected and the rest is transmitted through the powder. Energy from the light is only reflected away from the powder at the powder’s surface and is independent of the thickness of the powder. As the light penetrates into the powder bed, the optical power is attenuated as a portion of the light is absorbed by the powder, transmitting the rest. By measuring the attenuation of the transmitted light through powder layers of varying thickness, the amount of absorbed light can be gauged.

To conduct this experiment the TI OPT101 photodiode was also used in this experiment to measure the intensity of the light. It was sputter coated with gold-palladium to darken the front face in order to increase the maximum level of intensity the photodiode can read before becoming saturated. The photodiode was permanently fixed to a glass plate which was then leveled and focused to the projector’s image. The photodiode and glass plate were then fixed to a three axis CNC machine where a razor blade was fixed to one of the axis. A layer of powder was manually deposited on top of the photodiode and glass plate and the CNC machine carried out automated code which moved the powder, glass plate and photodiode under the razor blade, spreading uniform layers of powder at varying thicknesses. After each layer of powder was deposited, the CNC machine positioned the photodiode and glass plate beneath the projector where a completely white uniform image was projected. The projector was lifted to a distance of approximately 0.5m away from the photodiode. This decreased the power density by enlarging the projection image to prevent sintering from occurring and to prevent the photodiode’s output voltage from being saturated. The photodiode’s output was then recorded and correlated with varying powder layer thicknesses as seen below in Figure 6.

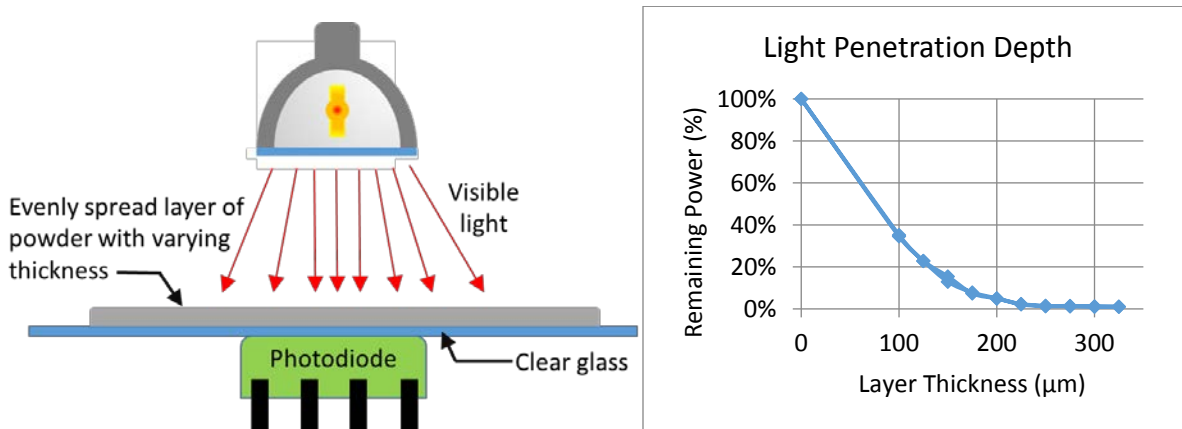


Figure 6 - left) schematic of system for measuring light intensity at varying powder depths, right) optical intensity profile.

In order to determine what the minimum layer thickness is, layers of powder were spread with the CNC machine in 25 μm increments. The PA2202 powder which was used for these tests have a mean particle size of 55 μm. The minimum layer thickness which could be repeatably spread without smearing was found to be 100 μm. This means the thinnest layer which can be repeatably spread is about two particles thick. Layers which are 100 μm thick are standard in the additive manufacturing industry. It is small enough to provide decent Z resolution but not so small that build times are drastically increased or spreading uniform layers becomes difficult. In this first 100 μm of powder, 65% of the light has been absorbed by the powder and at 200 μm, or 2 typical layers into the powder, only 5% of the light remains. These are promising results as a majority of the optical power is absorbed quickly in the first layer leaving only a small portion of the light to penetrate further into the powder. This could be advantageous as the transmitted light which is absorbed by the second layer thickness could aid in fusing new layers of powder together.

### SINGLE LAYER PART TESTING

To maximize the strength of any type of part or material, the porosity needs to be kept at a minimum. This allows the bulk of the material to bear and evenly distribute any loading forces. To maximize the load carrying capability, the strength should also be maximized. Since porosity and strength are important characteristics of any material, they should be investigated to determine the optimum manufacturing parameters which will maximize the performance of the part. In this study, components under different levels of sintering are cross sectioned and viewed under an SEM and are also tested for maximum load carrying capability in a tensile testing machine.

#### **SEM Evaluation of Porosity and Thickness**

To create parts with adequate strength, the powder must fully melt and densify during sintering. To analyze the degree of densification, four test coupons were sintered under varying degrees of exposure time at the maximum optical intensity. These test coupons were sintered on a powder bed 1.5mm thick (27 times the mean particle diameter). This case should approximate the sintering of the first layer of a part. They were then submerged in a bath of liquid nitrogen and broken in half to create a brittle fracture with a nearly flat fracture surface. These components were

then sputter coated with gold-palladium to create a conductive surface and imaged with a Hitachi S800 SEM as seen below in Figure 7.

Exposure times below 1.5s produced parts that were too weak to be handled and are not imaged. As seen in Figure 7a, little particle necking took place during sintering with individual particles clearly visible through the entire part thickness, resulting in a low degree of densification and low part strength. The bottom layers show little evidence of sintering. As the exposure time is increased, the particles reach higher temperatures (and thus lower viscosity) and have longer time to densify as seen in Figure 7b. As the exposure time is further increased, the parts further densify and the thickness of the dense region increases as the molten nylon coalesces with neighboring particles. At longer exposures, a smooth surface layer is formed with few visible pores. Increasing exposure times increases the thickness of this layer. After 3s the layer is approximately 100  $\mu\text{m}$  thick, which is encouraging for the formation of multilayer parts. However, longer exposures also produce curling of the edges of the parts and is discussed in more detail below.

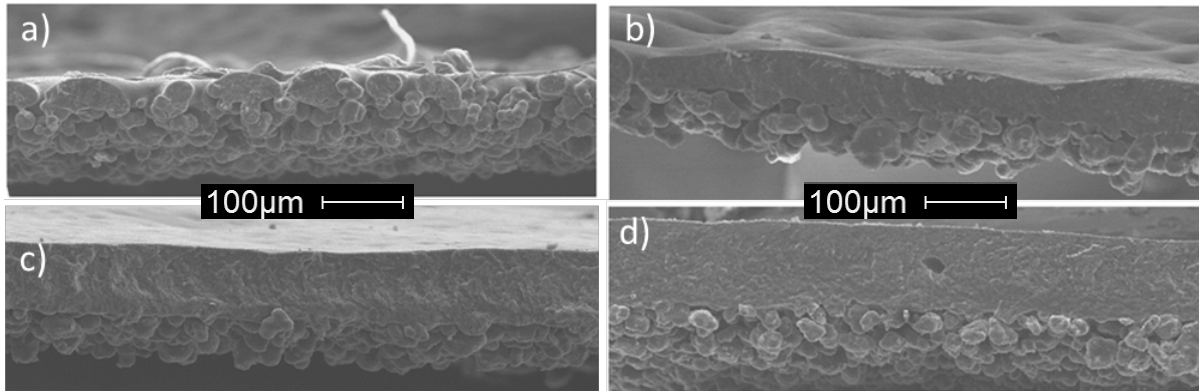


Figure 7 - All components were sintered with 100% intensity and are shown at 100x magnification. The exposed surface is on top in all images. a) 1.5s exposure b) 1.75s exposure c) 2.0s exposure d) 3s exposure.

## Tensile Testing

In order to analyze the strength of parts produced with projection sintering technology, single layer tensile test specimens were created using a single exposure. Various sintering tests were conducted and tested in accordance to ASTM standard D638-10 and the combinations of intensity and time are summarized in Table 1. The tensile specimen geometry is similar to the standard, however it has been scaled down to fit the maximum exposure size and the gauge width was increased to increase the total breaking force. The projected image had an overall length of 22.5mm and a gauge width of 7.3mm. All parts were produced with a single exposure. Thickness was determined by the heating time/intensity combination used. After removal from the powder bed, the back of each specimen was lightly brushed to remove loose non-load bearing powder. The specimen thickness was measured with a dial indicator whose contact tip was replaced with a blunted 27 gauge needle. The blunt needle was used to enable measurement of curled samples. The specimens were measured on the long axis centerline at three locations and averaged. Each of these tests were conducted on a MTS 810 hydraulic tensile testing machine.

Table 1 – Fabrication parameters and results of tensile testing coupons, three specimens were tested at each parameter set.

Test Constant	Intensity	Exposure Time (s)	Power Density (W/cm <sup>2</sup> )	Energy Dose (J)	Avg Thickness (μm)	Avg Breaking Force (N)
Intensity	100%	1	1.97	7.3	161 ± 15	N/A
	100%	1.25	1.97	9.125	212 ± 39	N/A
	100%	1.5	1.97	10.95	220 ± 15	5.9 ± 3.5
	100%	2	1.97	14.6	288 ± 15	22.1 ± 3.6
	100%	2.5	1.97	18.25	381 ± 0	35.5 ± 5.4
	100%	3	1.97	21.9	483 ± 0	49.5 ± 3.0
	100%	4	1.97	29.2	656 ± 26	62.2 ± 5.5
	100%	5	1.97	36.5	627 ± 44	53.5 ± 19.3
	100%	10	1.97	73	1080 ± 13	195.2 ± 9.5
	100%	15	1.97	109.5	1325 ± 15	226 ± 27.9
Exposure Time	100%	3	1.97	21.90	445 ± 38	22 ± 10
	90%	3	1.78	19.71	406 ± 13	29.6 ± 5.9
	80%	3	1.58	17.52	322 ± 19	22.7 ± 4.1
	70%	3	1.38	15.33	246 ± 15	13.8 ± 1.8
	60%	3	1.18	13.14	246 ± 15	4.5 ± 1.7
	50%	3	0.99	10.95	191 ± 13	N/A
	40%	3	0.79	8.76	N/A	N/A
Energy Dose	100%	2	1.97	15	229 ± 13	9.7 ± 5
	90%	2.22	1.78	15	237 ± 19	12.1 ± 1.6
	80%	2.5	1.58	15	254 ± 13	9.6 ± 7.1
	70%	2.86	1.38	15	301 ± 15	2.4 ± 2.1
	60%	3.33	1.18	15	296 ± 7	3.1 ± 0.8
	50%	4	0.99	15	292 ± 0	9.8 ± 3

During these tests the components which were sintered for a short period of time remained flat but were also of insufficient strength to be handled. Few could be extracted from the powder bed without damage. Specimens which were well sintered showed a large degree of curling directly after exposure in the powder bed. This made it difficult to measure the cross sectional width in the gauge length. The forces recorded during tensile testing were not able to be converted to stress values because of this. Since forces do not demonstrate a material property, they are used here only for relative comparison.

Three different tensile tests were conducted. For the first set of tests, 30 tensile test bars were created, 3 for each of the 10 test parameters. For these tests, the light intensity was held constant at the maximum value. Exposure times were increased from 1-15s which also increased the overall energy input into each specimen (energy dose). By increasing the exposure time (and energy dose), the powder is allowed longer periods of time to densify. As the exposure is maintained for longer periods of time, the powder is able to reach higher temperatures, and thus lower viscosities. This allows the material to flow more readily and to coalesce with neighboring particles. Increasing exposure time has the effect of creating thicker, denser and therefore, stronger parts. However, considerable curling was occurring with exposures over 1.5s as seen in Figure 8 below. Since the specimens that were produced with 1.5s exposure times only show a minimal amount of strength, the warping mechanism will need to be determined and corrected in order to create functional 2D or 3D parts. With 10s of exposure or more, the part's edges warped upwards during sintering, uncovering the powder beneath it which was then also sintered to the part, creating a perimeter. With a 10s exposure, the time and temperature were sufficient to cause stress relaxation which allowed the part to lay flat again.



Figure 8 – Tensile specimens made with the maximum intensity a) 1.5s exposure and 10.95J of energy, b) 2.5s exposure and 18.25J of energy, c) 15s exposure and 109.5J of energy.

For the second tests, the exposure time was held constant at 3s and the intensity was decreased from 100% to 40%. Three tensile bars were made for each of the 7 test conditions, for a total 21 tensile bars. The exposure time for this test was chosen because it produced a part of decent strength but produced excessive warping. By decreasing the intensity by 10% for each sample set, the optimal time-intensity setting could be identified. As the intensity was decreased (which also decreased the energy dose) lower strength, thinner parts were produced. The optimal intensity value was found to be at 70% intensity and can be viewed in Figure 10 below. This created a part of decent strength with minimal warping. The lowest possible intensity for this exposure time to produce parts that can be handled was identified to be at 60%. Parts below this value left a darkened discoloration in the powder but crumbled upon handling.



Figure 10 – Tensile specimens made with a 3s exposure, a) 100% intensity with 3J of energy, b) 70% intensity with 2.1J of energy, c) 50% intensity with 1.5J of energy.

During the third set of testing, the intensity was decreased from 100% to 50% while the total input energy was maintained. This required the exposure time to increase as the intensity decreased to maintain the overall energy dose. This had an effect of greatly decreasing the amount of warping but at the cost of reducing the load carrying capability. However, the change in the maximum achievable force and thickness varied much less between tests than with the previous two tests. This indicates that the time and intensity are inversely proportional to some degree. If the intensity or the time must be changed, then the other variable should change in the opposite direction as well to maintain the energy dose. It is evident from the pictures seen below, in Figure 10, that less sintering is occurring in the parts which have been exposed for a longer period of time at a lower intensity. However, a lot of variation was seen in these measurements, especially for the 60% and 70% intensity specimens. This could be caused by a non-ideal situation with the samples during handling, loading or during the sintering process. In order to reduce the variation, a higher energy dose would increase the ease of measurement and make the specimens less likely to be damaged before testing. Eighteen tensile bars were made for this set of testing but still requires more work to fully understand. Conducting this test at higher energy doses could help in understanding this effect. Additionally, adapting Andrew's number (measure of relative energy density) or the energy melt ratio (comparison of actual to theoretical sintering conditions) to projection sintering could aid in finding the correct parameter set to get high quality parts [19, 20].



Figure 9 - Tensile specimens made with the same energy dose, a) 4s exposure and 50% intensity, b) 3.33s exposure and 60% intensity, c) 2s exposure and 100% intensity.

## **CONCLUSION**

A new area based sintering technology and system are created to aid in analyzing the role of time and optical intensity in polymer sintering. This system is capable of sintering entire 2D cross sections with a single quick exposure. The modified projector used in this study was examined for accuracy in exposure time and calibrated to accurately control the intensity. The nylon 12 powder was also characterized to determine melt temperature and visible light absorption. This understanding is critical in the development of the new proposed method of sintering.

Projection based sintering can potentially expand the capable materials in the sintering field beyond the commonly used nylon. This system could aid in the understanding of sintering kinetics outside the realm of high heating rates. It is also the first step in creating a system capable of creating 3D printed parts with this technology. This large area sintering technology is modular and can be scaled to industrial sized machines. Additional or higher power projectors could be used to sinter with higher heating rates or over larger areas. Fast refresh rates of projectors also allow for dynamic control over spatial temperature distributions within the exposure area. However, many obstacles exist, including warping and correcting for a nonuniform distribution of light across the exposure field. More work still needs to be completed to fully understand the role time and intensity play in sintering kinetics and how it effects the overall part performance. Additionally, future work will have to be conducted to evaluate the effect long exposures have on the minimum feature size that can be obtained with these systems. This preliminary work suggests that energy input per unit area may still be a useful process parameters but may need some adjustments when used for longer processing times.

## References

- [1] T. T. Wohlers, *Wohler's Report: 3D Printing and Additive Manufacturing State of the Industry*. Fort Collins: Wohlers Associates, 2015.
- [2] R. D'Aveni, "THE 3-D PRINTING REVOLUTION," *Harvard Business Review*, vol. 93, pp. 40-48, 2015.
- [3] K. Maney. (2016) How 3-D Printing Will Make Manufacturing in America Great Again; Factories will essentially get broken up, scattered and made local.  
Available: <http://ezproxy.lib.usf.edu/login?url=http://search.ebscohost.com/login.aspx?direct=true&db=edsgao&AN=edsgcl.448774686&site=eds-live>
- [4] T. P. V. Ketterl, Y.; Arnal, N.C.; Stratton, J.W.I.; Rojas-Nastrucci, E.A.; Cordoba-Erazo, M.F.; Abdin, M.M.; Perkowski, C.W.; Deffenbaugh, P.I.; Church, K.H.; Weller, T.M., "A 2.45 GHz Phased Array Antenna Unit Cell Fabricated Using 3-D Multi-Layer Direct Digital Manufacturing," *Microwave Theory and Techniques, IEEE Transactions on Antennas and Propagation*, vol. 63, pp. 4382-4394, 2015.
- [5] I. Gibson, D. Rosen, and B. Stucker, *Additive manufacturing technologies : 3D printing, rapid prototyping, and direct digital manufacturing*: New York, NY : Springer, 2015. Second edition., 2015.
- [6] S. O. Akande, K. W. Dalgarno, J. Munguia, and J. Pallari, "Assessment of tests for use in process and quality control systems for selective laser sintering of polyamide powders," *Journal of Materials Processing Technology*, vol. 229, pp. 549-561, 3// 2016.
- [7] P. Peyre, Y. Rouchausse, D. Defauchy, and G. Régnier, "Experimental and numerical analysis of the selective laser sintering (SLS) of PA12 and PEKK semi-crystalline polymers," *Journal of Materials Processing Tech.*, vol. 225, pp. 326-336, 11/1/November 2015 2015.
- [8] M. Launhardt, A. Wörz, A. Loderer, T. Laumer, D. Drummer, T. Hausotte, *et al.*, "Detecting surface roughness on SLS parts with various measuring techniques," *Polymer Testing*, vol. 53, pp. 217-226, 8// 2016.
- [9] R. W. S Rösenberg, F. Knoop, H.-J. Schmid, M. Gessler, H. Pfisterer, "Controlling the Quality of Laser Sintered Parts Along the Process Chain," in *Solid Free Form Symposium* Austin, Texas, 2012.
- [10] A. Greco and A. Maffezzoli, "Polymer melting and polymer powder sintering by thermal analysis," *Journal of Thermal Analysis & Calorimetry*, vol. 72, pp. 1167-1174, 2003.
- [11] R. D. Goodridge, C. J. Tuck, and R. J. M. Hague, "Laser sintering of polyamides and other polymers," *Progress in Materials Science*, vol. 57, pp. 229-267, 1/1/2012 2012.
- [12] S. K. Tiwari, S. Pande, S. Agrawal, and S. M. Bobade, "Selection of selective laser sintering materials for different applications," *Rapid Prototyping Journal*, vol. 21, p. 630, 11// 2015.
- [13] G. Dörner and R. W. Lang, "Influence of various stabilizer systems on the ageing behavior of PE–MD—I. Hot-water ageing of compression molded plaques," *Polymer Degradation and Stability*, vol. 62, pp. 421-430, 12// 1998.
- [14] S. H. Hamid, *Handbook of polymer degradation. [electronic resource]*: New York : Marcel Dekker, c2000. 2nd ed., rev. and expanded / edited by S. Halim Hamid., 2000.

- [15] B. Haworth, N. Hopkinson, D. Hitt, and X. Zhong, "Shear viscosity measurements on Polyamide-12 polymers for laser sintering," *Rapid Prototyping Journal*, vol. 19, p. 28, 01// 2013.
- [16] C. T. Bellehumeur, M. K. Bisaria, and J. Vlachopoulos, "An experimental study and model assessment of polymer sintering," *Polymer Engineering & Science*, vol. 36, pp. 2198-2207, 1996.
- [17] C. Tonhauser, D. Wilms, Y. Korth, H. Frey, and C. Friedrich, "Entanglement Transition in Hyperbranched Polyether-Polyols," *Macromolecular Rapid Communications*, vol. 31, p. 2127, 12/15/ 2010.
- [18] "PA2202 Material Data Sheet," E. GmbH, Ed., ed, 2009.
- [19] M. Vasquez, B. Haworth, and N. Hopkinson, "Methods for quantifying the stable sintering region in laser sintered polyamide-12," *Polymer Engineering and Science*, p. 1230, 2013.
- [20] D. M. J. Williams, C. Deckard, "Selective Laser Sintering Part Strength as a Function of Andrew Number, Scan Rate and Spot Size," in *Solid Free Form Fabrication Symposium*, Austin, Texas, 1996.